PARSIVEL snow observations: A critical assessment

PARSIVEL Snow Observations: A Critical Assessment

ALESSANDRO BATTAGLIA AND ELKE RUSTEMEIER

Meteorological Institute, University of Bonn, Bonn, Germany

ALI TOKAY

Joint Center for Earth Systems Technology (JCET), University of Maryland, Baltimore County, Baltimore, and NASA Goddard Space Flight Center, Greenbelt, Maryland

ULRICH BLAHAK

Institute for Meteorology and Climate Research, Universität Karlsruhe/Forschungszentrum, Karlsruhe, Germany

CLEMENS SIMMER

Meteorological Institute, University of Bonn, Bonn, Germany

(Manuscript received 20 May 2009, in final form 10 September 2009)

ABSTRACT

The performance of the laser-optical Particle Size Velocity (PARSIVEL) disdrometer is evaluated to determine the characteristics of falling snow. PARSIVEL's measuring principle is reexamined to detect its limitations and pitfalls when applied to solid precipitation. This study uses snow observations taken during the Canadian Cloudsat/Cloud-Aerosol Lidar and Infrared Pathfinder Satellite Observation (CALIPSO) Validation Project (C3VP) campaign, when two PARSIVEL instruments were collocated with a single two-dimensional disdrometer (2-DVD), which allows more detailed observation of snowflakes. When characterizing the snowflake size, PARSIVEL instruments inherently retrieve only one size parameter, which is approximately equal to the widest horizontal dimension (more accurately with large snowflakes) and that has no microphysical meaning. Unlike for raindrops, the equivolume PARSIVEL diameter—the PARSIVEL output variable—has no physical counterpart for snowflakes.

PARSIVEL's fall velocity measurement may not be accurate for a single snowflake particle. This is due to the internally assumed relationship between horizontal and vertical snow particle dimensions. The uncertainty originates from the shape-related factor, which tends to depart more and more from unity with increasing snowflake sizes and can produce large errors. When averaging over a large number of snowflakes, the correction factor is size dependent with a systematic tendency to an underestimation of the fall speed (but never exceeding 20%).

Compared to a collocated 2-DVD for long-lasting events, PARSIVEL seems to overestimate the number of small snowflakes and large particles. The disagreement between PARSIVEL and 2-DVD snow measurements can only be partly ascribed to PARSIVEL intrinsic limitations (border effects and sizing problems), but it has to deal with the difficulties and drawbacks of both instruments in fully characterizing snow properties.

1. Introduction

Detailed snow observations, which provide estimates of both the intensity of snowfall and the spectral characteristics of snowflakes, are urgently needed to improve microphysical parameterizations in numerical weather prediction models and to develop remote sensing–based algorithms for retrieving snow rates. Woods et al. (2007) showed that changes in the assumed mass–diameter and velocity–diameter relationships of snowflakes significantly modified the distribution of precipitation, as predicted by a mesoscale model in a mountainous environment. Liu (2008), Hong (2007), and Hiroshi (2008) demonstrated

Corresponding author address: Alessandro Battaglia, Meteorological Institute, University of Bonn, Auf dem Hügel, 20, 53121 Bonn, Germany.
E-mail: batta@uni-bonn.de

DOI: 10.1175/2009JTECHA1332.1

the importance of ice crystal habits when computing backscattering properties at millimeter wavelengths for remote sensing purposes.

Snow observations have been performed in the recent past, mainly by two-dimensional video disdrometers (2-DVDs), such as the 2-DVD described in Kruger and Krajewski (2002) or the Hydrometeor Velocity and Shape Detector (Barthazy et al. 2004; Barthazy and Schefold 2006), with the former (latter) having two orthogonal (horizontal) beams. Based on measurements in eastern Colorado, Brandes et al. (2007) investigated the behavior of the snow bulk densities and tried to characterize the particle size distributions (PSDs) by looking for relationships among the different Gamma-function fitting parameters. Brandes et al. (2008) proposed power laws relating aggregate terminal velocities and temperatures at the ground. They ascribed the observed rise in speed with temperature to accretion by rimming (Pruppacher and Klett 1997). Very recently, Newman et al. (2009a) presented the Snowflake Video Imager, which stores the snowflake perimeter and provides the maximum length between any two points as a characteristic size parameter. The Snowflake Video Imager–based PSD parameterization was then used to validate the 915-MHz profiler-based PSD retrieval in snow (Newman et al. 2009b). Unlike two-dimensional optical disdrometers, the Snowflake Video Imager cannot measure the fall velocity, but it can provide a more detailed image of individual snowflakes.

Earlier snow measurements based on the Particle Size Velocity (PARSIVEL) disdrometer (an instrument originally designed for liquid precipitation; Löffler-Mang 1998) have been reported by Löffler-Mang and Joss (2000). A good agreement between C-band snow radar reflectivity and the reflectivity derived from PARSIVEL measurements was found by Löffler-Mang and Blahak (2001), but only after some tuning of a mass–size relationship. Yuter et al. (2006) confirmed that, as claimed by the manufacturer, PARSIVEL can be exploited as a present weather sensor because of its capability to distinguish rain, snow, and wet snow. Eight precipitation types are actually included in the built-in software. A renewed interest in snow measurements with such an optical disdrometer has recently appeared in the frame of the Canadian Cloudsat/Cloud-Aerosol Lidar and Infrared Pathfinder Satellite Observation (CALIPSO) Validation Project (C3VP) and of the Towards an Optimal-estimation Snow Characterization Algorithm (TOSCA) campaigns.

The major obstacle in the interpretation of PARSIVEL data for snow events lies in the instrument retrieval rationale, which assumes raindrop-like particles. Thus, a critical assessment of the potential of the PARSIVEL instrument in quantitatively characterizing snowflake properties is mandatory. The instrument retrieval of PARSIVEL is based on the following assumptions (U. Blahak 2009, unpublished manuscript):

(i) Particles have spheroidal shapes, like raindrops.
(ii) Particles are falling with their axis of symmetry vertically aligned (horizontal orientation of major axis).
(iii) Particles partially seen by the measurement beam (margin fallers) cannot be discerned and are treated as nonmargin fallers. Such particles are recorded too small and too slow. The assumption is that their mean influence on PSDs and integral quantities can be accounted for by a simple correction of the effective measuring area. Newer PARSIVEL models (produced by the company OTT after 2004) detect margin fallers by two additional photo diodes.
(iv) Particles have extinction properties with respect to the monochromatic laser light similar to raindrops (i.e., particles are almost opaque).
(v) The vertical component of the fall velocity determines solely the measured duration of the particle signals; that is, there is no effect of horizontal transport through the laser beam.
(vi) Only one particle is in the beam at one certain time.

This paper discusses the implications of the first three assumptions in determining quantitative information about snow. These assumption in particular affect the computation of the characteristic size, the fall speed, and the snowflake size distribution. The aforementioned C3VP campaign provided a unique opportunity to investigate these aspects. During C3VP, different disdrometers were installed at the Center for Atmospheric Research Experiments (CARE) site in southern Ontario, Canada (see Fig. 1) from October 2006 to March 2007, a period when abundant numbers of synoptic and lake-effect-based snow is observed.

2. Description of the PARSIVEL disdrometer

PARSIVEL is a laser-optical disdrometer manufactured formerly by PMTech and in more recent times by OTT, and it is intended for hydrometeor size and fall-speed measurements. PARSIVEL can measure sizes up to about 25 mm and uses 32 size classes of different widths, spread over 0–26 mm. The lowest two size classes are not used at all because of their low signal-to-noise ratio. Registration starts only at the lower size bound of class 3 (0.25 mm). We will refer to the derived particle dimension as "PARSIVEL size." Hydrometeors, especially snowflakes, generally have nonspherical shapes; only for raindrops, the PARSIVEL size can be approximately

FIG. 1. Picture of the CARE site located 80 km north of Toronto at 44.23°N, 79.78°W at a height of 249 m MSL. The 2-DVD (pinpointed by the arrow) and the two PARSIVEL disdrometers (within the dashed ellipse) are visible in the center and on the right side (private picture taken by Peter Rodriguez, Environment Canada).

interpreted as the diameter of a sphere with equivalent volume. The smallest and largest detectable fall velocities are about 0.2 and 20 m s^{-1}, respectively. The velocity is subdivided into 32 nonequidistant classes, starting from 0 and reaching up to 22.4 m s^{-1} (upper margin of class 32). Thus, PARSIVEL stores particles in 32×32 matrices with a temporal resolution of 1 min (with the new OTT version capable of setting the ''integration interval'' to 10 s).

The instrument generates a flat, horizontal 650-nm laser sheet with a surface A of 27 mm $\times$ 180 mm and a height of 1 mm. A single photo diode converts the received light into an electric voltage, which is converted to a digital output signal. To eliminate the effect of background light (e.g., sun), the laser is periodically pulsed, and the output signal is discretely sampled in time as the difference between two consecutive ''on'' and ''off'' state of the laser system. This signal changes whenever a hydrometeor or other objects large enough intercepts the beam. The degree of dimming is assumed as a measure of hydrometeor size; thus, it is assumed to be proportional to shadow of the particle. The fall velocity is calculated from the particle size (by assuming a fixed relationship between horizontal and vertical dimensions) and the time period during which the light sheet is measurably affected by the particle. The effect on the signal voltage caused by two falling spherical particles of different sizes is illustrated in Fig. 2. Note that the depicted output signal is obtained by subtracting the undisturbed background signal from the signal affected by the particle and inverting it. The continuous blue lines represent the particle dimming, and the stars are the actual discrete samples recorded by the instrument.

In the PMTech version deployed during C3VP, the output voltage is sampled at 10 kHz (OTT PARSIVELs have a sampling rate of 25 kHz); that is, one sample is taken every 0.1 ms (see diamonds in Fig. 2). From the sampled output signals, the maximum signal is estimated from the highest output and its left and right neighbors by parabolic interpolation (see black line in Fig. 2, right). For the example in the right panel (a 2-mm raindrop falling at 6 m s^{-1}) only four samples are available. This example illustrates clearly that the maximum of the interpolating parabola is a much better estimate of the true maximum compared to the sampled maximum.

The time duration of the signal Δt is estimated from the time the signal is above half of the maximum signal Δt_{50}; Δt_{50} is reasonably well estimated from a linear interpolation between the two sample pairs next to the half value of the estimated maximum amplitude (see the dashed lines in Fig. 2, left, which are hard to see because of the closeness with the real signal). The relation between Δt and Δt_{50} has been tuned to raindrops measurements; in fact, Δt cannot be detected very accurately, given the small number of samples, especially for fast raindrops. The conversion from Δt_{50} to Δt is performed via a transfer function, which has been determined by curve fitting to a Monte Carlo ensemble of simulated particle signals (following the first and second assumptions, as stated in section 1). Snowflakes typically fall at speeds between 1 and 2 m s^{-1} (Locatelli and Hobbs 1974). Snowflakes larger than 1 mm in diameter produce 13–20 sampled voltages, enough to properly determine Δt without the need of reverting to Δt_{50} (e.g., see Fig. 3). Nevertheless, PARSIVEL uses the procedure described here to estimate Δt.

3. PARSIVEL retrieval rationale

Thanks to the coauthorship of one of the PARSIVEL software developers (Dr. Blahak), we could get a better knowledge about the PARSIVEL retrieval rational. PARSIVEL's size and speed retrieval concept has been tuned to raindrops. As such, particles below 1-mm equivalent sphere diameter $D_{\text{eq}}^{\text{PAR}}$ are assumed to be spheres, where the superscript PAR stands for PARSIVEL; its presence reminds that this is a quantity related to the PARSIVEL rationale. We underline that, only for raindrops, it can be interpreted as an equivolume sphere diameter. In the range from 1 to 5 mm, all particles are assumed to be horizontally oriented oblate spheroids with axial ratio a_r^{PAR} (defined as the ratio between height and width) linearly varying from 1 to 0.7. For particles

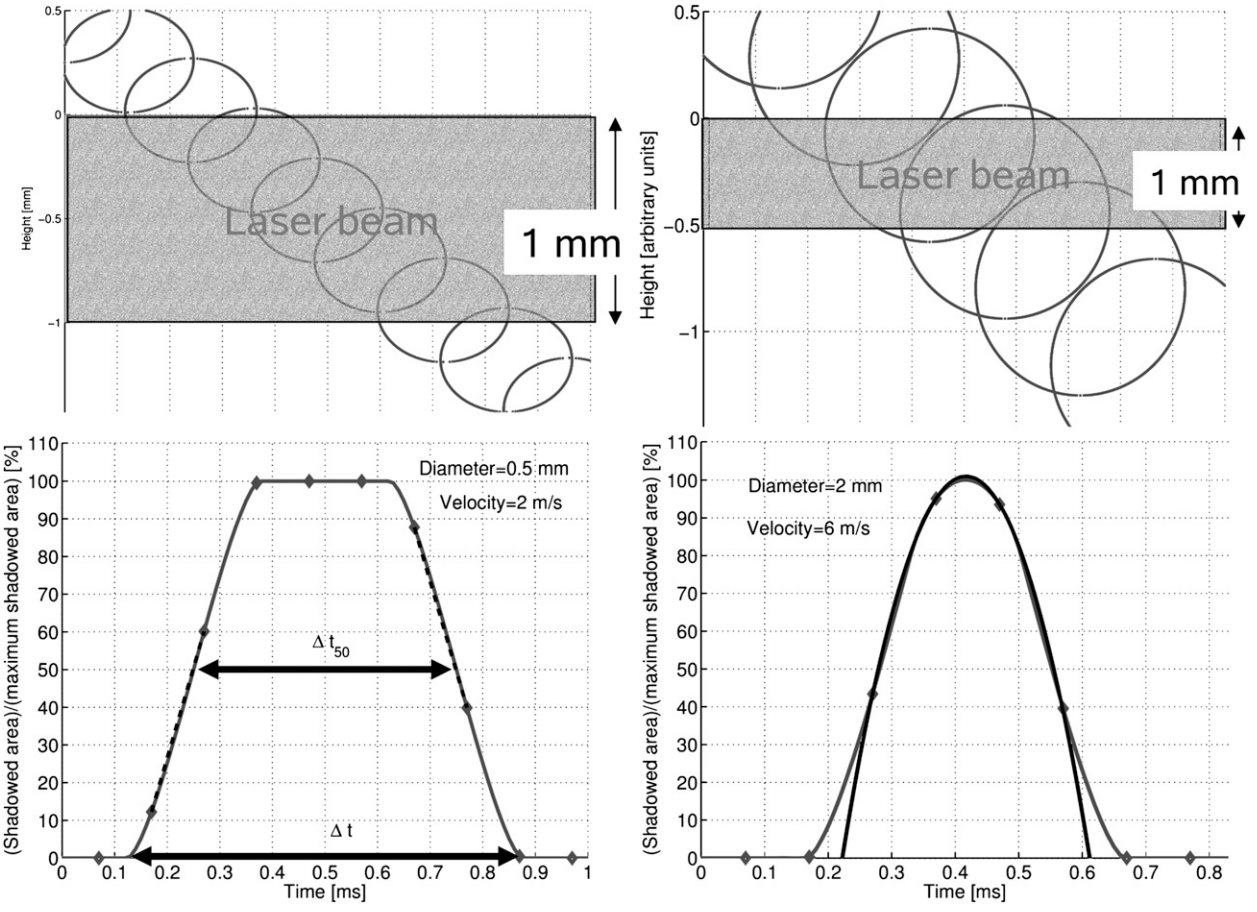

FIG. 2. Schematic diagram showing the influence of the size and of the velocity of two particles passing through the PARSIVEL beam on the output voltage. The diamonds represent the discrete PARSIVEL 10-kHz samples; continuous lines indicate the effective continuous signal produced by the particle dimming, normalized to its peak value $F_{\max}$. (left) A 0.5-mm-diameter sphere (the small deformation is due to graphical problems) falling at 2 m s^{-1}. The dashed line is shown to exemplify the technique adopted to compute Δt_{50} (by linear interpolation). (right) A 2-mm-diameter sphere falling at 6 m s^{-1}. The black continuous line is shown to exemplify the technique adopted to estimate the maximum signal (by parabolic interpolation).

with diameters above 5 mm, the axial ratio is kept constant at a value of 0.7:

$$a_r^{\mathrm{PAR}} \equiv \begin{cases} 1 & D_{\mathrm{eq}}^{\mathrm{PAR}} \le 1\,\mathrm{mm} \\ 1.075 - 0.075 D_{\mathrm{eq}}^{\mathrm{PAR}} & 1\,\mathrm{mm} < D_{\mathrm{eq}}^{\mathrm{PAR}} < 5\,\mathrm{mm} \\ 0.7 & D_{\mathrm{eq}}^{\mathrm{PAR}} \ge 5\,\mathrm{mm} \end{cases}, \tag{1}$$

with $D_{\mathrm{eq}}^{\mathrm{PAR}}$ in millimeters. When applied to other hydrometeors (e.g., snowflakes), this becomes a more or less arbitrary assumption. Any departure from raindrop-like shapes will produce errors in the estimated fall velocity and diameter. We refer to particles falling into these three ranges as small, intermediate, and large particles.

Note that there is a hidden switch in the software to change the internally assumed shape from oblate spheroid to purely spherical (e.g., for industrial applications). This is typically never activated during meteorological measurements.

a. Size parameter retrieval

Given the 1-mm height h of the beam, the maximum area $F_{\max}$ shadowed by a horizontally oriented oblate spheroid is given by

$$F_{\max} = \begin{cases} \pi AB & B \le \dfrac{h}{2} \\ 2AB\left[\arcsin\left(\dfrac{h}{2B}\right) + \dfrac{h}{2B}\sqrt{1 - \left(\dfrac{h}{2B}\right)^2}\right] & B > \dfrac{h}{2} \end{cases}, \tag{2}$$

where A and B are the major and minor semiaxis of the spheroids, respectively. An example for both situations (small and large spheroids, respectively) is shown in Fig. 4a. Note that for large B values ($\gg h/2$) the shadowed

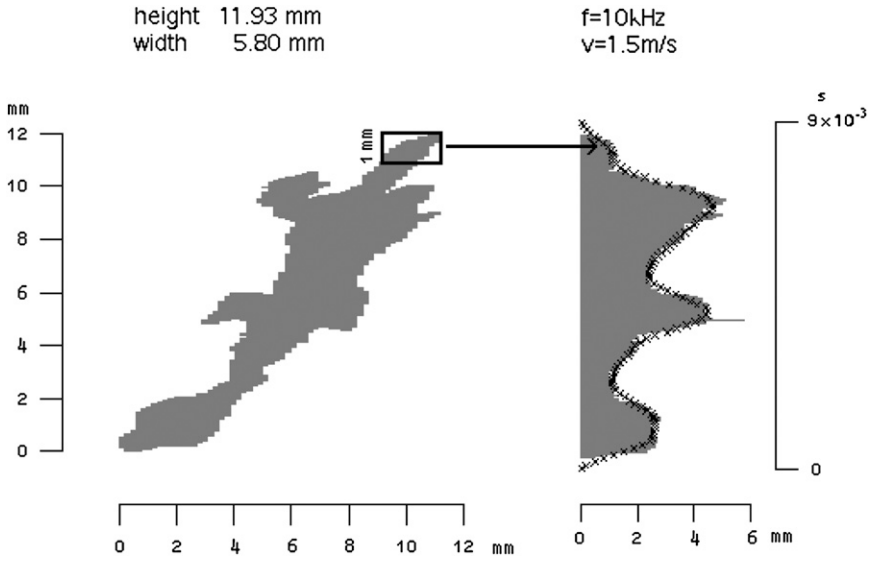

FIG. 3. (left) 2-DVD front view of a large snowflakes. (right) Simulated PARSIVEL-shadowed area with around 80 samples (crosses) as a function of time (vertical axis).

area [Eq. (2)] becomes $2A \times h$ (i.e., the area of a rectangle).

The PARSIVEL signal, which is the reduction of the output voltage, is directly related to the shadowed area. The shadowed area is converted to the PARSIVEL size $D_{\text{eq}}^{\text{PAR}}$, assuming an oblate spheroid of volume $^4/_3\pi A^2 B$ ($B = a_r A$). Accordingly, $D_{\text{eq}}^{\text{PAR}}$ is computed via $D_{\text{eq}}^{\text{PAR}} = 2Aa_r^{1/3} = 2Ba_r^{-2/3}$. Using this, Eq. (2) is inverted to compute $D_{\text{eq}}^{\text{PAR}}$. Snowflakes may, however, have rather complicate shapes. Relations between cross section and equivolume diameter for a sphere and a rectangle are given in Fig. 5 along with the relation used by PARSIVEL. We can conclude that, for arbitrary particles, the only dependable variable measured by PARSIVEL is the maximum shadowed area of the particle, which can be retrieved from the shown PARSIVEL size by reversing the arrows in Fig. 5. Which size parameters can we retrieve from the maximum shadowed area? As an

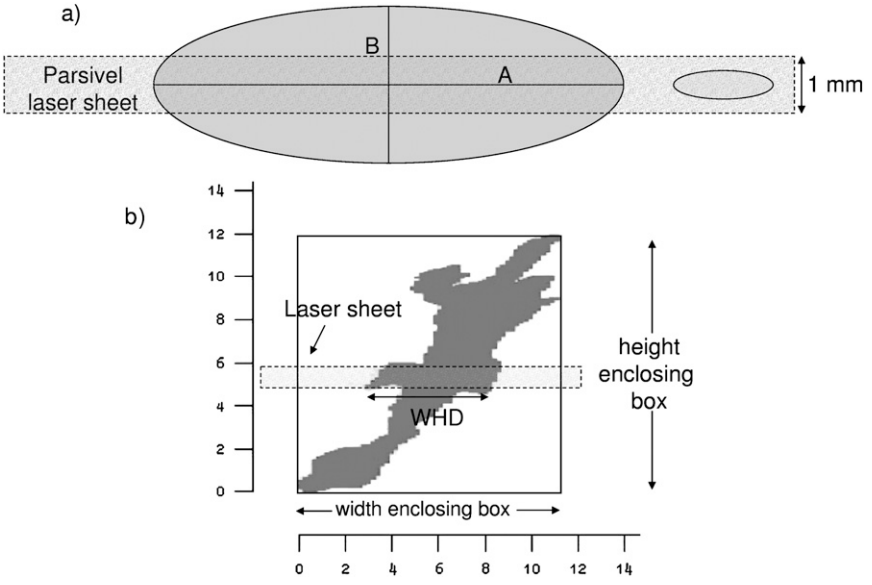

FIG. 4. (a) Schematic diagram of a small and a large spheroidal particle shadowing the 1-mm-thick PARSIVEL beam. (b) Schematic measuring example for a snowflake.

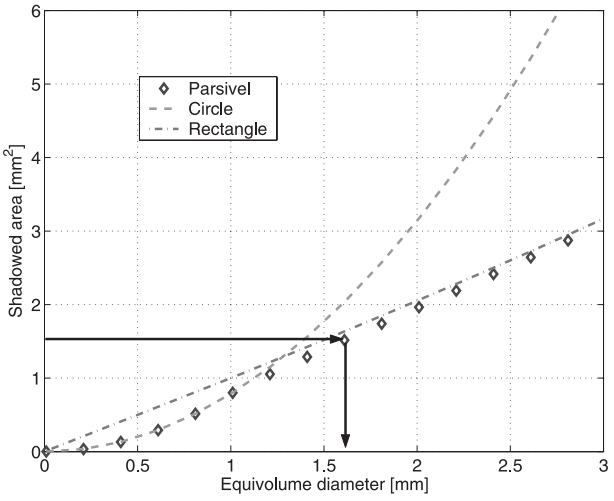

FIG. 5. Equivolume diameter $D_{\rm eq}^{\rm PAR}$ vs maximum shadowed area $F_{\max}$ [see Eq. (2)] as estimated by the PARSIVEL software. Note that for $D_{\rm eq}^{\rm PAR} < 1$ mm the result coincides with the shadow of a circle (because $h = 1$ mm coincides with the upper threshold diameter for assumption of spherical particles in $a_r^{\rm PAR}$ and at large $D_{\rm eq}^{\rm PAR}$ the shadowed area corresponds to that of a rectangle with width equal to $2A = D_{\rm eq}^{\rm PAR}/(a_r^{\rm PAR})^{1/3}$ and height equal to 1 mm. The arrows indicate how the equivolume diameter is internally estimated by PARSIVEL.

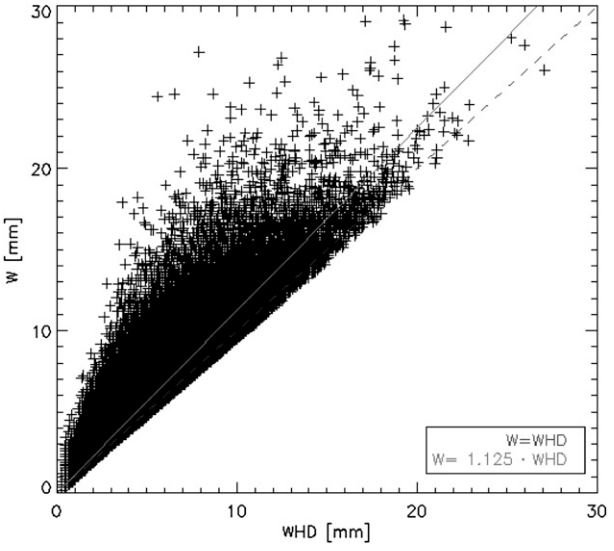

FIG. 6. Scatterplot between WHD (mm) and width of the enclosing box W (mm) for one million snowflakes as measured by the 2-DVD probe during the C3VP campaign. The solid line represents the best rms fitting linear relationship between the two quantities. The dashed line is the one-to-one line.

important but not exhaustive example, we analyze the signal of particles whose plane-projected area can be described as an ellipse with major (minor) semiaxis A (B). To generate a realistic variability of snowflake silhouettes, we varied the axial ratios between 1 and 0.2 and the ellipse tilting angle between 0° and 90°. For an ellipse with its major axis tilted by an angle θ, Eq. (2) becomes

$$F_{\max} = \begin{cases} \pi AB & H \le h \\ 2AB\left[\arcsin\left(\dfrac{h}{H}\right) + \dfrac{h}{H}\sqrt{1-\left(\dfrac{h}{H}\right)^2}\right] & H > h, \end{cases} \tag{3}$$

with $H = 2\sqrt{A^2\sin^2\theta + B^2\cos^2\theta}$ being the height of the ellipse enclosing box. When H becomes much larger than the vertical extend of the PARSIVEL beam, the shadowed area becomes $4(AB/H) \times h$, with $4(AB/H)$ being the widest horizontal dimension (WHD) of the ellipse. This quantity is smaller than the width of the enclosing box (W). Figure 4b shows as an example a snowflake having a width of the enclosing box equal to 11.5 mm and WHD approximately equal to 6 mm. The difference between the width of the particle enclosing box (W) and the WHD increases with the axial ratio and is maximum at tilting angles around 45° (e.g., for axial ratios equal to 0.2, the ratio WHD/W is about 0.4, such as in the former example). Both quantities are only equal when particles fall with tilting angles equal to 0° or 90°. Thus, the difference between WHD and W has to be kept in mind, in addition to the fact that neither of these two variables has a direct microphysical meaning (like the maximum dimension or the equivolume/equimass diameter of the snowflakes). Figure 6 illustrates the relationship of both quantities for a sample of almost one million snowflakes measured by the 2-DVD probe during the C3VP campaign (C3VP and 2-DVD are described in section 4). For the 2-DVD sample, about 20% of the flakes have WHD larger than 2 mm, whereas about 6% of the flakes measured by the PARSIVEL have $D_{\rm eq}^{\rm PAR}$ larger than 2 mm. On average, W is 10%–15% larger than WHD, but many snowflakes exhibit much larger departures. We can, however, estimate WHD from the stored equivolume diameter $D_{\rm eq}^{\rm PAR}$ by adopting the assumptions concerning the axial ratio of Eq. (1) as

$$\mathrm{WHD}_{\rm retr}^{\rm PAR} \equiv \frac{D_{\rm eq}^{\rm PAR}}{(a_r^{\rm PAR})^{1/3}}, \tag{4}$$

which simply follows from the definition of $D_{\rm eq}^{\rm PAR}$ as sphere equivalent diameter of an assumed horizontally aligned spheroid with axis ratio $a_r^{\rm PAR}$ and WHD = $2A$. Thus, for large particles, WHD is simply obtained by multiplying $D_{\rm eq}^{\rm PAR}(1/0.7)^{1/3} = 1.126$. This method will produce good estimate of WHD only when the falling

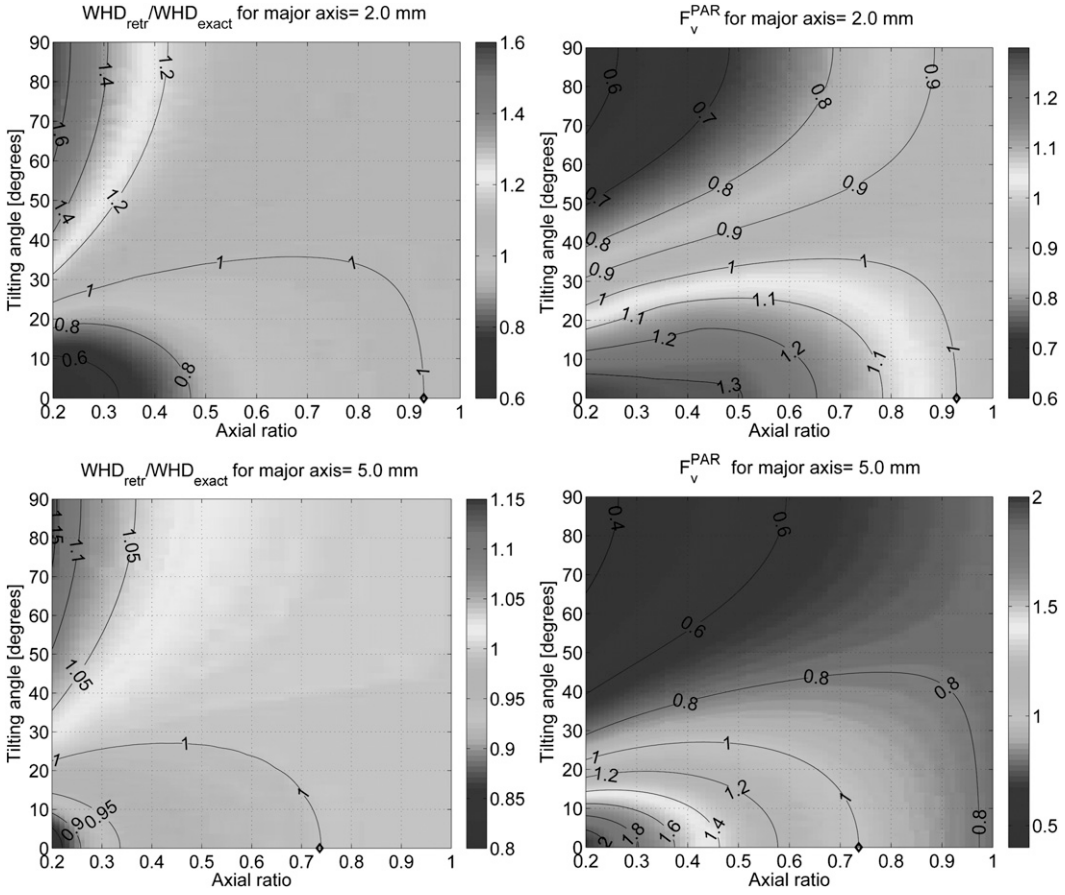

FIG. 7. (left) Ratios between retrieved and exact WHD for an ellipse with major axis equal to (top) 2 and (bottom) 5 mm. (right) The function $F_{\upsilon}^{\mathrm{PAR}}$, which compares in Eq. (7) for an ellipse with major axis equal to (top) 2 and (bottom) 5 mm. The black diamond on the x axis indicates the axial ratios retrieved by the PARSIVEL software for the given major axis.

snow crystal or flake falls horizontally aligned and its shape is close to the assumed raindrop-like shape. In general, this condition is not satisfied. For a given maximum dimension of a particle (e.g., a given major axis), the discrepancy between retrieved and exact WHD becomes larger when the axial ratio is departing from that internally assumed by the PARSIVEL and when the orientation diverts from the horizontal. As an example, we present (Fig. 7, left) the ratios between retrieved [i.e., by calculating $F_{\max}(A, B, \Theta)$, inverting Eq. (2) to get $D_{\mathrm{eq}}(F_{\max})$, and then using Eq. (4) to calculate $\mathrm{WHD}_{\mathrm{retr}}^{\mathrm{PAR}}$] and exact (i.e., geometrically calculated from A, B, and the tilting angle Θ) WHD for ellipses with major axis equal to 2 and 5.0 mm. The axial ratio assumed by PARSIVEL is indicated by the diamond symbol. When the particle size increases, the quality of the retrieval procedure becomes independent from the axial ratio assumption and from the orientation of the crystal. For instance, for an ice crystal with major axis equal to 5 mm, the WHD retrieved by Eq. (4) has at most a 20% error, despite its oblateness and its orientation (Fig. 7, bottom left).

b. *Fall-speed retrieval*

The beam dimming duration Δt (see Fig. 2) is related to the effective fall speed of the particle v_{eff} and the height of the enclosing box H (see Fig. 4b) via

$$v_{\mathrm{eff}} = \frac{H + h}{\Delta t}. \tag{5}$$

This quantity cannot, however, be measured directly by the instrument, but we can assume $H_{\mathrm{est}}^{\mathrm{PAR}} = D_{\mathrm{eq}}^{\mathrm{PAR}}$ (when the spherical option is adopted) and $H_{\mathrm{est}}^{\mathrm{PAR}} = D_{\mathrm{eq}}^{\mathrm{PAR}}(a_r^{\mathrm{PAR}})^{2/3}$ (like for our and for typical meteorological measurements, which are hereafter considered). Thus, we have to write

$$v_{\mathrm{est}}^{\mathrm{PAR}} = \frac{H_{\mathrm{est}}^{\mathrm{PAR}} + 1\,\mathrm{mm}}{\Delta t}, \tag{6}$$

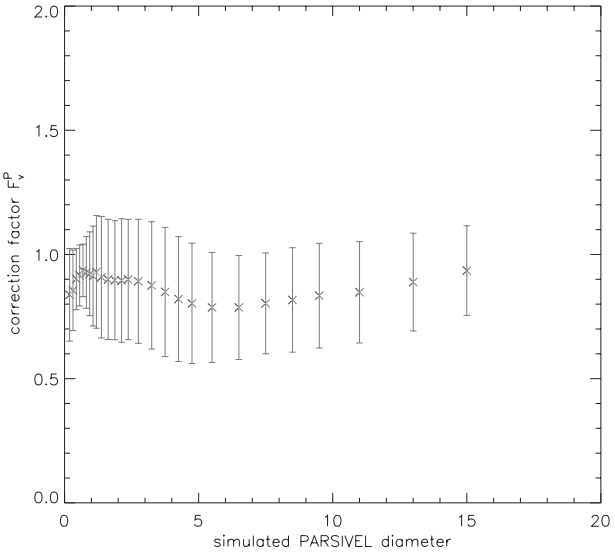

FIG. 8. Mean (crosses) and std devs (bars) of the correction factor F_v^{PAR} [see definition in Eq. (7)] as a function of $D_{\mathrm{eq}}^{\mathrm{PAR}}$ (mm). About one million 2-DVD snowflake observations have been categorized into different widest horizontal dimension classes. A relation of the form $H_{\mathrm{est}}^{\mathrm{PAR}} = D_{\mathrm{eq}}^{\mathrm{PAR}}(a_r^{\mathrm{PAR}})^{2/3}$ is assumed.

which, by eliminating Δt from (5) and (6), relates to the true velocity via

$$v_{\mathrm{est}}^{\mathrm{PAR}} = \frac{H_{\mathrm{est}}^{\mathrm{PAR}} + h}{H + h} v_{\mathrm{eff}} \equiv F_v^{\mathrm{PAR}} v_{\mathrm{eff}}, \tag{7}$$

with F_v^{PAR} being a correction factor. Obviously, the velocities of snowflakes with heights smaller than those retrieved by PARSIVEL software $H_{\mathrm{est}}^{\mathrm{PAR}}$ will be overestimated and vice-versa. Note that, in reality, F_v^{PAR} is slightly different, because PARSIVEL actually measures Δt_{50} and estimates Δt from it, a procedure that also uses the raindrop-like shape assumption.

The right panels of Fig. 7 depict the behavior of this correction factor as a function of the axial ratio and of the orientation angle of the ellipsoidal projected area, with major axis equal to 2.0 and 5.0 mm. A strong dependence of the error, which can reach 100% (i.e., $F_v^{\mathrm{PAR}} = 2.0$), on the axial ratios and on the orientation is evident. The increase of the particle size enhances the weight of the correction factor.

For the C3VP database, we have computed the correction factor F_v^{PAR} by evaluating 2-DVD observations of about one million snowflakes (Fig. 8). In Eq. (7), H is a direct output of 2-DVD, whereas $H_{\mathrm{est}}^{\mathrm{PAR}}$ is computed from $\mathrm{WHD}^{\text{2-DVD}}$. The PARSIVEL tends to slightly underestimate the fall speed of small crystals for all sizes. For very large snowflakes, the mean underestimation in fall speed, which can reach values of 20%, tends to cancel out. By looking at the underestimation regions in the right panels of Fig. 7, this suggests a tendency of large snowflakes to have axial ratios closer to one and fall more randomly oriented.

4. Border and particle shape effects

To understand the importance of particle shape deviations from the assumed specific spheroidal shape and the impact of border effects, a simulation study has been conducted by exploiting collocated 2-DVD and PARSIVEL data collected during the C3VP campaign. The 2-DVD instrument provides much more detailed shape information by the use of two orthogonal image projections of the hydrometeor silhouette (e.g., width and height of the enclosing box and equivolume diameter from both cameras). Because of a two camera recording system (line scanner), it measures the fall velocity independently from the shape. The 2-DVD has about twice the sampling area of PARSIVEL (100 mm $\times$ 100 mm), and thus it is less sensitive to border effects (Fig. 9). Nonetheless, the 2-DVD has its own pitfalls, especially in the presence of strong winds (during C3VP, horizontal winds of 4–5 m s^{-1} were quite frequent). For the low-profile 2-DVD deployed during C3VP, wind effects are expected to be not as strong as in the first version of the 2-DVD (Nespor et al. 2000). Unfortunately, no studies of wind effects on snow measurements with the low-profile 2-DVD are available at the present. Despite this, for the C3VP campaign we observed no systematic trend with the horizontal winds (not shown). 2-DVD presents difficulties in the matching procedure of the particles in the two cameras and cannot resolve particles smaller than 0.2 mm. Finally, an additional source of problems can be related to the breakup of snowflakes and drifting of fragments on the large flat surface of the low-profiler 2-DVD. As a matter of fact, 2-DVD cannot be considered an absolute reference system.

We simulated PARSIVEL observations based on a long-lasting snow event observed by 2-DVD and compared the simulations with collocated PARSIVEL measurements. Each snowflake detected by the 2-DVD is simulated to fall into the 2-DVD sampling area via a Monte Carlo procedure, which determines its random position. The generated snowflakes represent a synthetic sampling of the actual snowstorm with duration $t_{\mathrm{snowstorm}}$. If the snowflake (or part of it) falls within the PARSIVEL sampling area (Fig. 9), then it is counted as registered by the PARSIVEL. The PARSIVEL shadowed area is computed either as the 2-DVD silhouette area (when the height of the snowflake is less than 1 mm) or by using the second expression in Eq. (2), with $2A$ and $2B$ corresponding to the WHD and the height of the enclosing box measured by 2-DVD. The two 2-DVD

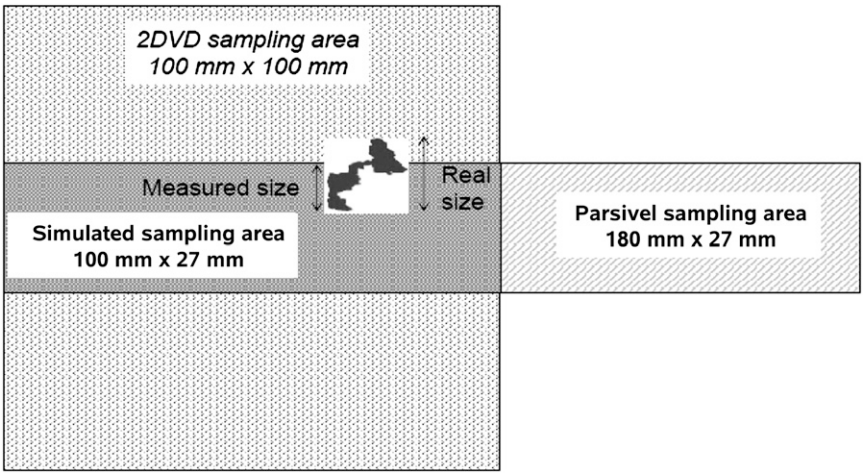

FIG. 9. Schematic diagram with the top view of the 2-DVD, PARSIVEL, and simulated measuring planes. To demonstrate the border effects, a snowflake, falling into the 2-DVD sampling area and only partially in the PARSIVEL beam, is shown.

cameras provide two perpendicular side views of the same snowflake. If only part of the snowflake intercepts the PARSIVEL sampling area, then the shadowed area is reduced accordingly (see Fig. 9). An additional simulation is performed without accounting for this effect; we refer to this simulation as the case ''without border effects.'' Then, $D_{\rm eq}^{\rm PAR}$ is computed from the shadowed area by the PARSIVEL lookup table. The PARSIVEL velocity $v_{\rm est}^{\rm PAR}$ is estimated by Eq. (7) by assuming that $v_{\rm eff}$ coincides with the velocity measured by the 2-DVD. If M_j snowflakes fall within a certain ''PARSIVEL diameter'' class centered around $D_{\rm eq}^{\rm PAR}(j)$ with width $\Delta D_{\rm eq}^{\rm PAR}(j)$, the PSD N_V is computed as follows:

$$N_V[D_{\rm eq}^{\rm PAR}(j)] = \frac{1}{A_{\rm sampling}[D_{\rm eq}^{\rm PAR}(j)]\Delta D_{\rm eq}^{\rm PAR}(j)\, t_{\rm snowstorm}} \times \sum_{k=1}^{M_j} \frac{\mathcal{R}_{\text{2-DVD}}(k)}{v_{\rm est}^{\rm PAR}(k)}, \quad (8)$$

where $\mathcal{R}_{\text{2-DVD}}$ is a renormalization coefficient introduced to account for the reduced 2-DVD sampling area of large snowflakes and $A_{\rm sampling}$ is the PARSIVEL sampling area. If all margin fallers were detected and eliminated, the sampling area would be $A_{\rm sampling} = 180\,{\rm mm}\{27\,{\rm mm} - 2A[D_{\rm eq}^{\rm PAR}(j)]\}$; if all margin fallers were measured with their correct size and velocity, then $A_{\rm sampling} = 180$ mm $\times$ 27 mm. In reality, margin fallers happen but are not detected as such by the PMTech PARSIVELs, so the ''truth'' must be somewhere in between. Having in mind rain drops with $D_{\rm eq} \ll$ width of light sheet, the simple correction $A_{\rm sampling} = 180\,{\rm mm}[27\,{\rm mm} - D_{\rm eq}^{\rm PAR}(j)/2]$ has been chosen in the software, disregarding the slight difference between $2A$ and $D_{\rm eq}^{\rm PAR}$.

The simulated PSD and fall velocity as a function of $D_{\rm eq}^{\rm PAR}$ is then compared with the PARSIVEL measurements. An example is shown in Fig. 10 for an event during 20–21 January 2007 ($t_{\rm snowstorm} = 26$ h), which was characterized by temperatures lower than -6°C and by relative humidities above 85%. More than 600 000 snowflakes were recorded by the 2-DVD instrument, thus sampling errors introduced by the small disdrometer sampling areas can be neglected. As a confirmation of this, data from the two PARSIVEL instruments were compared. The PSD of the two PARSIVELs deployed at less than 1-m distance (see Fig. 1) are indeed very close (green stars and crosses in Fig. 10) and confirm our model. The PSDs measured by the PARSIVELs and by the 2-DVD are plotted versus $D_{\rm eq}^{\rm PAR}$ and WHD, respectively. The first evident result (common to all observations during the C3VP campaign) is that the 2-DVD has the tendency to measure more large snowflakes and less small snowflakes than the PARSIVELS. This discrepancy is partly due to the different size parameters used to plot the PSDs and to border effects. In fact, the Monte Carlo–simulated PARSIVEL PSDs based on the 2-DVD measurements (triangles) resemble more closely the observed PARSIVEL PSDs (stars and crosses). When swapping one size parameter WHD for the other $D_{\rm eq}^{\rm PAR}$, the WHD 2-DVD distribution (blue diamonds) turns clockwise [roughly pivoting around the point (7.5 mm, 3 mm^{-1} m^{-3})], thus approaching the PARSIVEL results in all size bins and becoming close to the red triangles. The red triangles are now directly comparable with the

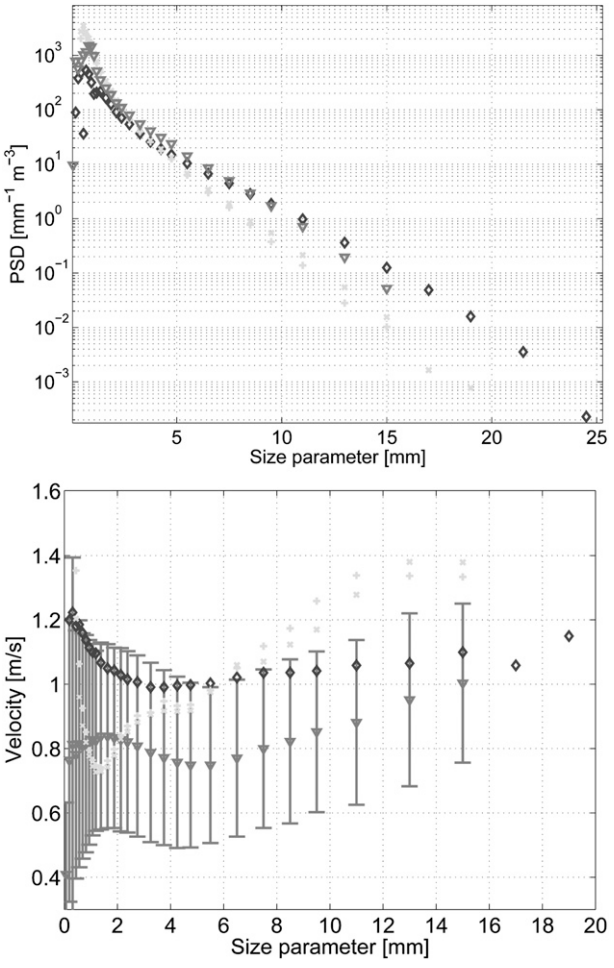

FIG. 10. (top) PSDs as measured by the 2-DVD as a function of the WHD (diamonds) and by two PARSIVEL instruments (crosses and stars) close each other as a function of D_{eq}^{PAR}. For ease of comparison, the Monte Carlo–simulated PARSIVEL PSD (triangles) is plotted as a function of D_{eq}^{PAR} as well. (bottom) Symbols as in (top) for fall speeds. For the Monte Carlo–simulated results (triangles), error bars corresponding to the std dev are added. Similar magnitudes are found for the other lines.

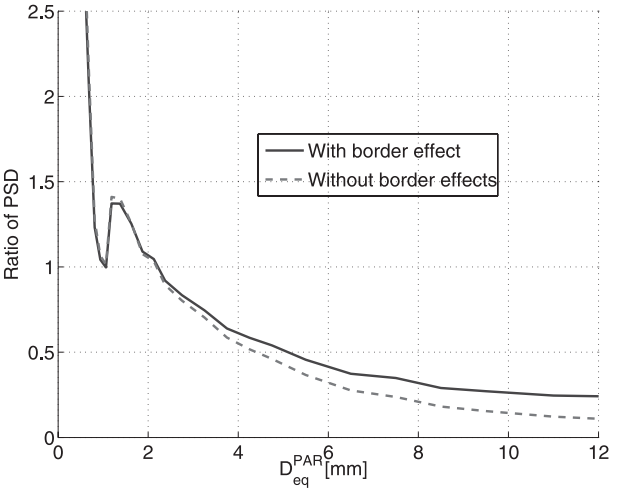

FIG. 11. Ratio between measured PARSIVEL (mean of the two available instruments) and Monte Carlo–simulated PSD. Four snowstorms are included for a total of almost one million snowflakes.

PARSIVEL results, because the PSDs are plotted versus the same size parameter.

The border effect tends to decrease the counting of large snowflakes (with WHD $>$ 10 mm) in favor of smaller particles. The effect becomes critical for counting within the large-size bins because, as a result of its smaller sampling area, the PARSIVEL cannot register snowflakes with WHD larger than 27 mm (which corresponds to $D_{eq}^{PAR} = 24$ mm). Given the exponential-like PSD shape and the few countings of large particles, the counterbalancing in small-size bins will not be noticeable. The ratio between the Monte Carlo–simulated and the PARSIVEL-measured PSDs is depicted in Fig. 11. By comparing the two curves in Fig. 11, it becomes clear that border effects produce no consequences in the PSD for snowflakes with $D_{eq}^{PAR} \approx 2$ mm but reduce the measured PARSIVEL PSD by around 50% for $D_{eq}^{PAR} \approx 10$ mm. The peak around $D_{eq}^{PAR} \approx 1$ mm is clearly an artifact resulting from the assumptions adopted when computing the PARSIVEL shadowed area. The discrepancy between PARSIVEL and 2-DVD is still present even when border effects are accounted for, with a systematic overestimation for small sizes ($D_{eq}^{PAR} < 2$ mm) and an underestimation for large diameters. For $D_{eq}^{PAR} > 5$ mm, the PARSIVEL-derived PSD is less than half of the 2-DVD PSD. This difference cannot be ascribed to border effects, because this has been already accounted for. Border effects produce a further depletion of large snowflakes (cf. dashed and continuous lines in Fig. 11) but cannot explain the drastic underestimation of PARSIVEL PSD at large sizes.

The simulated velocities (Fig. 10, bottom) do not agree quite well with those measured by the PARSIVEL. The factor F_v^{PAR} only accounts for some of the discrepancies between PARSIVEL and 2-DVD observations for small sizes but actually pushes the 2-DVD results even further away from the PARSIVEL solution at large sizes ($D_{eq}^{PAR} > 3$ mm). Curiously, the velocity of small snowflakes seems to increase as the size parameter decreases below 1 mm. This departs from the usual expected power-law trend and seems to pinpoint at some systematic pitfall of the PARSIVEL and the 2-DVD or at the presence of freezing droplets, at least during part of the event. This issue requires additional investigations.

Compared to 2-DVD, PARSIVEL tends to measure faster snowflakes, especially at large sizes. We speculate

that this is partly caused by the procedure, which estimates Δt from Δt_{50} (which again is based on raindrop-like behavior). Snowflakes occur very often as aggregates with many branches. The corresponding PARSIVEL signal will then present several separated peaks and troughs, as demonstrated in Fig. 3. The PARSIVEL software will interpret this signal as coming from different particles (three in the depicted case) with smaller Δt, hence velocities higher than the true ones. Given the larger number of output voltage samples per snowflake, a direct estimate of Δt (e.g., by extrapolation fitting) is believed to be more precise, and a modification of the PARSIVEL software should be considered for snow. Such a modification will, however, impair the instrument capability of detecting two coinciding particles when they are not aligned along the beam axis and their time signal does not overlap too much. However, this would affect only a small percent of typical snow cases.

In addition, the mismatch between the two measurements can be attributed to inherent difficulties of both instruments when operated in windy conditions, which were typical during the measurement campaign. In such conditions, because of preferentially horizontal instead of vertical transport through the laser beam, the falling snowflake can travel only part of the 1-mm laser height fully shadowing the beam. This implies that sizes of large snowflakes (with vertical dimensions much larger than the beam height) are systematically underestimated and speeds are somewhat overestimated by PARSIVEL, even if the particles obey the assumed shape relation. On the other hand, as pinpointed by Nespor et al. (2000), although reduced in its current low-profile configuration, the 2-DVD can be affected by significant errors because of turbulent eddies developing within the measuring volume, thus altering the fall speed of the particles and maybe entirely hindering particles from entering the 2-DVD enclosure. This additional error of both instruments adds to the error resulting from deviations of snowflakes from the assumed shape and may account for the unexplained errors in Fig. 10 (bottom).

5. Discussion and conclusions

We can draw some preliminary conclusions. Such conclusions cannot be definitive, simply because we do not have an absolute reference to calibrate with. Although we consider 2-DVD as a reference, 2-DVD has its own shortcomings. Only an extensive cross comparison of various instruments in different snow conditions and broadening our horizons beyond the 2-DVD and PARSIVEL instruments will ascertain the effective potential of in situ measurements in characterizing the microphysical properties of snow. We can summarize our findings in the following subsections.

a. PARSIVEL size parameter

When characterizing the snowflake size, PARSIVEL instruments inherently retrieve only one size parameter, which is approximately equal to the widest horizontal dimension WHD. This quantity underestimates the width of the enclosing box (Fig. 6) and even more the maximum dimension of the snowflake (example in Fig. 4). The current PARSIVEL output variable $D_{\text{eq}}^{\text{PAR}}$ has no physical counterpart. The translation of $D_{\text{eq}}^{\text{PAR}}$ to WHD can be performed via Eq. (4) based on the first assumption (see section 1). As a rule of thumb, for large particles when shadowing does not depend on the height of the particle, the derivation of WHD from $D_{\text{eq}}^{\text{PAR}}$ will be quite accurate. For small particles, large uncertainties are caused by the unknown shape and orientation of the particle.

b. Fall velocity

Measuring snowfall velocity with the PARSIVEL presents difficulties because of the internally assumed relationship between horizontal and vertical snow particle dimensions. Most of the uncertainty originates from the shape-related factor F_v^{PAR} present in Eq. (7), which will tend to depart more and more from one with increasing snowflake sizes. For snowflakes observed during the C3VP campaign, F_v^{PAR} is, on average, lower than one but with a variance of 10%–20%. The comparison between the PARSIVEL simulated and measured data shows a PARSIVEL underestimation of fall velocities for small particles and an overestimation for large particles (up to 30%–40%). The accuracy of snow velocity measurements does not fulfill the requirements needed to develop snow velocity parameterizations.

c. Border effects

The PARSIVEL beam sheet has an area $A = 180\ \text{mm} \times 27\ \text{mm}$. Problems may occur in presence of big snowflakes when the ice crystal is falling in proximity to the light-sheet border. Such particles are counted as having smaller sizes and smaller fall velocities. Border effects obviously become relevant when the snowflake dimension approaches the minimum dimension of the PARSIVEL measuring area (i.e., 27 mm). The Monte Carlo simulation ascertains the decrease/increase in the large/small particle number caused by this effect. Because of the exponential shape of snow PSD, only the effect at large particle size is noticeable. For snowflakes with $D_{\text{eq}}^{\text{PAR}} \approx 2\,\text{mm}$, this effect produces no consequences in the PSD, whereas there is a reduction in the measured PARSIVEL PSD of around 50% for $D_{\text{eq}}^{\text{PAR}} \approx 10\,\text{mm}$. The

reduction factor can be linearly interpolated between these two values for intermediate values of $D_{\text{eq}}^{\text{PAR}}$.

d. Particle size distribution

The determination of PSD requires the computation of size and fall speed of the snowflakes. The errors in the retrieval of these quantities will propagate to the PSD. The disagreement between PARSIVEL and 2-DVD snow measurements can only be partly ascribed to border effects and to the different size variable used to define the PSD. Some additional pitfall in either the PARSIVEL or the 2-DVD has to be present.

PARSIVEL seems to overestimate the number of small snowflakes and to underestimate the number of large particles when compared to 2-DVD. The PSD underestimation at large sizes seems to be driven by size underestimation (more than by fall-speed overestimation). Note that this is particularly crucial for radar application (the reflectivity is mainly driven by large particles) and definitely limits the applicability of PARSIVEL in this field. Different factors can be the reasons for that. First, the signal produced by one single snowflake can be interpreted as caused by different snowflakes. This will tend to increase the number of small particles and the total snow particle density (which in our database is around 20% larger than the one measured by the 2-DVD). Second, horizontal transport produced by lateral wind will reduce the shadowed area and then produce a more skewed PSD, with more small and less large particles. Finally, the special extinction properties of the snowflakes (e.g., produced by holes in low-density flakes) at the laser frequency can also alter the relationship between voltage signal and shadowed area, causing underestimation of size, particularly for larger (thus, fluffy) particles. The possibility of a correction accounting for the different laser extinction between ice and water particles should be considered. A detailed investigation of such aspects is left to future work.

Acknowledgments. We would like to acknowledge V. N. Bringi and G. J. Huang of Colorado State University for providing 2-DVD data; D. Hudak, P. Rodriguez, and S. Brady of Environment Canada for organizing the field campaign and operating PARSIVELs during C3VP; P. G. Bashor of Computer Sciences Corporation for installing the PARSIVEL; M. Schwaller and R. Lawrence of NASA Goddard Space Flight Center for funding PARSIVEL operation; R. Kakar of TRMM Program Scientist for funding the research under Grant NNX07AF45G; and the Deutsche Forschung Gemeinshaft (DFG) for funding the work by E. Rustemeier in the frame of TOSCA and of the Transregio T32 project Pattern in Soil-Vegetation-Atmosphere-Systems: Monitoring, Modeling and Data Assimilation. We also acknowledge the very helpful and detailed remarks of the anonymous reviewers, who considerably improved the readability of the text.

REFERENCES

Barthazy, E., and R. Schefold, 2006: Fall velocity of snowflakes of different riming degree and crystal types. *Atmos. Res.,* **82,** 391–398.

——, S. Göke, R. Schefold, and D. Högl, 2004: an optical array instrument for shape and fall velocity measurements of hydrometeors. *J. Atmos. Oceanic Technol.,* **21,** 1400–1416.

Brandes, E. A., K. Ikeda, G. Zhang, M. Schönhuber, and R. M. Rasmussen, 2007: A statistical and physical description of hydrometeor distributions in Colorado snowstorms using a video disdrometer. *J. Appl. Meteor. Climatol.,* **46,** 634–650.

——, ——, G. Thompson, and M. Schönhuber, 2008: Aggregate terminal velocity/temperature relations. *J. Appl. Meteor. Climatol.,* **47,** 2729–2736.

Hiroshi, I., 2008: Radar backscattering computations for fractal-shaped snowflakes. *J. Meteor. Soc. Japan,* **86,** 459–469.

Hong, G., 2007: Radar backscattering properties of nonspherical ice crystals at 94 GHz. *J. Geophys. Res.,* **112,** D22203, doi:10.1029/2007JD008839.

Kruger, A., and W. F. Krajewski, 2002: Two-dimensional video disdrometer: A description. *J. Atmos. Oceanic Technol.,* **19,** 602–617.

Liu, G., 2008: A database of microwave single-scattering properties for nonspherical ice particles. *Bull. Amer. Meteor. Soc.,* **89,** 1563–1570.

Locatelli, J. D., and P. V. Hobbs, 1974: Fall speeds and masses of solid precipitation particles. *J. Geophys. Res.,* **79,** 2185–2197.

Löffler-Mang, M., 1998: A laser-optical device for measuring cloud and drizzle drop size distributions. *Meteor. Z.,* **79,** 53–62.

——, and J. Joss, 2000: An optical disdrometer for measuring size and velocity of hydrometeors. *J. Atmos. Oceanic Technol.,* **17,** 130–139.

——, and U. Blahak, 2001: Estimation of the equivalent radar reflectivity factor from measured snow size spectra. *J. Appl. Meteor.,* **40,** 843–849.

Nespor, V., W. F. Krajewski, and A. Kruger, 2000: Wind-Induced error of raindrop size distribution measurement using a two-dimensional video disdrometer. *J. Atmos. Oceanic Technol.,* **17,** 1483–1492.

Newman, A. J., P. A. Kucera, and L. F. Bliven, 2009a: Presenting the Snowflake Video Imager (SVI). *J. Atmos. Oceanic Technol.,* **26,** 167–179.

——, ——, C. R. Williams, and L. F. Bliven, 2009b: Snowflake size spectra retrieved from a UHF vertical profiler. *J. Atmos. Oceanic Technol.,* **26,** 180–199.

Pruppacher, H. R., and J. D. Klett, 1997: *Microphysics of Clouds and Precipitation*. 2nd ed. Kluver Academic, 954 pp.

Woods, C. P., M. T. Stoelinga, and J. D. Locatelli, 2007: The IMPROVE-1 storm of 1–2 February 2001. Part III: Sensitivity of a mesoscale model simulation to the representation of snow particle types and testing of a bulk microphysical scheme with snow habit prediction. *J. Atmos. Sci.,* **64,** 3927–3948.

Yuter, S. E., D. E. Kingsmill, L. B. Nance, and M. Löffler-Mang, 2006: Observations of precipitation size and fall speed characteristics within coexisting rain and wet snow. *J. Appl. Meteor. Climatol.,* **45,** 1450–1464.